DETECTING THE PRESENCE OF A PROXIMATE CELLULAR USER THROUGH DISTRIBUTED FEMTOCELL SENSING

A Thesis

by

PANKAJ PARAG

Submitted to the Office of Graduate Studies of
Texas A&M University
in partial fulfillment of the requirements for the degree of

MASTER OF SCIENCE

Approved by:

Chair of Committee,	Jean-François Chamberland-Tremblay
Committee Members,	Henry D. Pfister
	Srinivas G. Shakkottai
	Ronald G. Douglas
Head of Department,	Chanan Singh

December, 2012

Major Subject: Electrical Engineering

ABSTRACT

The current cellular industry is undergoing a huge paradigm shift from an old homogeneous one-tier network structure to a new heterogeneous two-tier structure with joint deployment of traditional macrocell base stations along with a relatively new small cell base stations, widely known as femtocells. Femtocells are low-powered, low-cost, user-deployed base stations meant to improve poor network coverage and, thereby, increase overall system capacity. As more and more femtocells are deployed, their spectrum usage and resulting interference become non-negligible. While using different operating frequency for femtocells is indeed possible, a co-channel deployment of these will increase spectral efficiency, a much sought design by cellular operators. In this thesis, a femtocell-based scheme is considered as a prospective means to enhance the performance of the current cellular infrastructure. In the adopted framework, the femtocell access point is tasked with connecting local femtocell users to the network operator without creating undue interference to cellular users. As such, the femtocell is required to cease communication when a nearby cellular user is present to prevent interference. In the envisioned paradigm, an access point possesses little information about the parent cellular base station. For instance, it may not know the individual channel gains, user locations or frequency allocations. To achieve this goal, femtocell users collectively act as sensing devices and are used to acquire data about local signal strength. This work shows that, despite having little knowledge of the operation of the macro environment, a femtocell can take advantage of the data provided by the acquisition devices and agility of the re-configurable antenna to gain insight about proximate cellular devices. The proposed inference scheme leads to a significant performance gain over oblivious femtocells. Experimental results are

provided to support this study and its conclusions.

ACKNOWLEDGMENTS

I would like to express my deepest appreciation to my advisory Dr. Jean-François Chamberland-Tremblay for his guidance, wisdom and patience. His support throughout was invaluable.

I am also grateful to my committee members Dr. Henry Pfister, Dr. Srinivas Shakkottai and Dr. Ronald Douglas for the interest they showed in my thesis and defense, their suggestions and time.

Many thanks to all my colleagues in the TCSP group who made working here enjoyable. I am especially grateful to Santhosh Vanaparthy, Sirisha Mantravadi, Gaurav Sharma for their continuous motivations and suggestions.

I am indebted to my brother Parimal Parag for his incredible support throughout my graduate studies. Finally, I would like to thank my parents for all the unconditional love and faith they have in me. I thank my family for their support and encouragement.

TABLE OF CONTENTS

LIST OF TABLES

LIST OF FIGURES

CHAPTER I

INTRODUCTION

Wireless communication and the Internet have become two important aspects of our day-to-day lives, drastically altering our lifestyle, interactions, culture and commerce. It would not be hyperbole to say modern life without these amenities would be unimaginable. It is amazing how things once considered a luxury (in the early 90s) have transformed into necessities in the modern world. The need for the fastest and most feasible way of communication can be attributed to the rise and growth of both wireless communication and the Internet.

The growth of Internet began with the development of point-to-point communication between terminals, which later expanded to computers, and subsequently led to further research in packet switching. Several protocols were put forth, which paved way for the development of internetworking, or network of networks. Standardization of TCP/IP in 1982, followed by the emergence of Internet service providers (ISPs) in 1980s and 1990s made the Internet accessible to the public. In parallel, the world witnessed major advances in VLSI design processes that enabled cheap manufacturing of computers. Both these success stories facilitated easy access to computers and the Internet for the masses. According to the Internet Telecommunication Union (ITU) [1], the penetration of the Internet has grown from approximately 9% ($\sim$ 500 millions) in 2001 to more than 30% ($\sim$ 2100 millions) worldwide by year 2011. This penetration has skyrocketed from below 30% in 2001 to 70% in the developed world by 2011.

The early communication method which was predominantly wired, relied heavily on telephone lines. Although wired communication is still the safest way for error free transmission, several improvements in latter years have made wireless transmission

more error tolerant. In this scenario, a wireless communication which requires much less infrastructure and gives an added benefit of portability and/or mobility has been considered. This mode of transmission is more lucrative and all these factors put together form the primary driving force behind the success of modern day wireless communication.

The earliest forms of wireless communication were radio and television transmissions. In this mode of telecommunication, there is a single transmitter and multiple receivers, a typical example of broadcast. Telegraph, on the other hand, is a shining example of unicast communication involving older wireless technologies. However, costly equipment made these approaches inaffordable for masses. Come 1950s and the improvements in technology, such as invention of transmitters led to smaller equipment and commercially viable two-way wireless communication.

An early instance of wireless telephony communication was seen in pre-cellular systems sometimes referred to as 0G. Technologies such as push to talk (PTT), mobile telephony system (MTS) were introduced in the 1960s as a part of it. It was slowly replaced by analog wireless technology, termed as 1G in 1980s. Since early 1990s, these technologies have largely been displaced by digital wireless technology known as 2G or second generation, which apart from delivering usual telephony, is also capable of carrying short text messages (SMS). The huge success of 2G is often credited to switching from analog technology to digital technology, which made the system more reliable, and made way for smaller portable handsets. In digital form, the signals are not corrupted by noise, use less bandwidth, and can be encrypted providing both easy transmission and security.

Later many advancements were made to 2G technologies to meet the market expectations, such as packet-switching and enhancement in data rates. While some of these technologies were built from scratch, most of them evolved from the older

2G technology. General Packet Radio Service (GPRS), better known as 2.5G, is capable of delivering data at the speed of 56-114 kbit/s. Enhanced Data rates for GSM Evolution (EDGE) or 2.75G was the next technology promising a data rate of 400 kbit/s to 1 Mbit/s.

At the same time, VLSI design improvements and chip fabrication methods have promoted cheap manufacturing of mobile handsets. According to the ITU [1] report, mobile-cellular telephony has jumped from around 15% ($\sim$ 1 billion) in 2001 to an outstanding 85% ($\sim$ 6 billions) in 2011 worldwide. Mobile usage in the developed world has gained tremendously from 45 per 100 in 2001 to more than 120 per 100 in 2011. The last decade has seen an explosive growth in sale of smartphones that incorporate special devices such as camera, global positioning system (GPS), gyroscope integrated into cellular phones on a single platform. These devices, which support data-consuming services such as audio-visual play, navigation, access to social network, and productivity suites, have fueled the demands for high speed data services. Even though the older 2G telephony system has been succeeded by the superior 3G, or third generation with increases data rates (up to maximus of about 28 Mbit/s), this unprecedented rise in demand for high-speed Internet access on a cellular device remains unfulfilled. Yielding to this demand, third generation wireless telephony will eventually be superseded by the 4G technology with even higher data throughput rates. More recently a cellular standard known as LTE, or Long Term Evolution, was introduced which provides data transfer speeds of up to roughly 300 Mbit/s.

A. Introduction of Small Cells

In each successive generation of mobile telephony since 1G, the basic theme of wireless communication is that every user equipment (UE) is assigned to a specific macrocell

base station (BS). This structure has remained a cornerstone in wireless communication and since its inception has enjoyed an overwhelming success. Even though highly successful, it evolved considerably over years and has gone undergone through some major overhauls. During its development in last two decades, several new ideas were proposed and implemented, including soft-handoffs, sectorization and universal frequency reuse.

With the introduction of high speed Internet access on cellular devices through technologies like 3G & 4G, the current cellular infrastructure is under lots of strain. Studies indicate that the traditional usage of cellular network, i.e. voice telephony has recorded a decrease in average revenue per user (ARPU) [2] while on-the-go data availability has recorded an extraordinary demand, indicated by increase in data ARPU [2].

This tremendous growth has prompted the wireless industry to investigate new ways of increasing system throughput and capacity compared to the current cellular infrastructure. A possible approach to this challenge is increasing the number of base stations and, thus, have each node handle fewer devices. Bandwidth can subsequently be reallocated from serving a large user population to supporting high-volume applications. Still, deploying additional base stations can be prohibitively expensive for the network operators. A more cost-effective way to address this issue of a rising demand is to enhance the transmitting-receiving capacity of the antennas by using multiple-input multiple-output (MIMO) technology or smart antennas. Pattern-dynamic antennas have been examined closely by the antenna and the statistical signal processing communities, leading to concrete improvements in the operation of cellular systems [3]. An in-depth cost saving analysis of smart antennas over conventional equipment is offered in [4]. More commercially profitable ways of improving system capacity are also being explored.

The quality of wireless transmissions is highly dependent on the proximity of the transmitting and receiving antennas. It is widely recognized that bringing the transmitter and receiver closer typically improves the signal-to-noise ratio and hence enhances overall performance. As such, small cells have been used to boost capacity.

In the last few years, the cellular industry has been shifting from a voice-centric, centrally planned, homogeneous paradigm to data-driven, packetized and distributed heterogeneous networks. In essence, a heterogeneous network is a tiered architecture consisting of a central macrocell base station working in coordination with other network elements, such as microcells, distributed antennas, relays, and picocells, to provide an adequate experience to end users. Innovations like auto-configuring, self-organizing networks [5] will reduce the load on macrocells and lower operational expenditure. A microcell is a network element served by a low-power cellular base station that covers a limited area such as a mall, a hotel, or a transportation hub. It uses power control mechanisms to limit the radius of its coverage area, which is typically less than two kilometers wide. A distributed antenna system is a network of spatially separated antennas connected to a common source via a transport medium. Recent studies show that more than 50% of the voice and 70% of data traffic originates indoors [6] where, typically, received signal strength is poor. Hence, along with increasing system capacity, there is an urgent need to address the problem of supporting data originating inside buildings. Deploying more macrocells, microcells and distributed antennas does not necessarily solve the problem of poor service to indoor users. Besides, the capital and operational expenditures involved are generally too high for any of the above methods to be commercially viable at high densities.

The current situation has sparked an interest in small base stations that are able to provide high data rates and supplement traditional macrocell base stations by enhancing indoor coverage in a cost-effective manner. In this regard, one of the

more interesting trends emerging from this scenario is the concept of femtocells [6, 7].

B. Femtocell

Femtocells are wireless data access points, usually installed by end users in homes or workplaces, that transmit their backhaul data through a broadband gateway to the core network of a cellular provider. The alternate interface can be cable, DSL (Digital Subscriber Line), Ethernet, fiber, etc. From the viewpoint of wireless providers, a femtocell deployed indoors has very little operational cost making it a very attractive option for improving the overall performance of network. Femtocells can provide exceptional cellular service in an indoor environment and can be installed in hot-spots and enterprise zones, which typically range in tens of meters. A femtocell connects to the cellular provider network directly through a broadband gateway, thus eliminating the reliance on the channel between the mobile user and its macrocell, which is often degraded by penetration losses associated with obstruction created by walls. A femtocell can devote most of its resources to achieve high SINR (signal-to-interference-plus-noise-ratio), providing better service to users. Femtocells also aide in increasing the battery life of handsets, because mobiles connected to a local femto access point do not have to reach a base station, an action which consumes much power. Furthermore, a femtocell can be designed as a plug-and-play device for easy use so that users are not deterred from using them. Femtocells are designed to act as a non-obtrusive, ancillary component of the cellular framework. More importantly, femtocells have extensive auto-configurable and self-optimization capabilities, allowing automatic integration with existing cellular 1infrastructures. Altogether, femtocells are beneficial to both cellular network operators and home users.

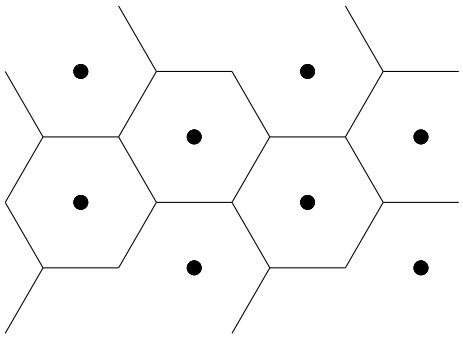

Fig. 1. The coverage area is divided into smaller cells with a base station in the center.

C. The Current Cellular Structure

In our current cellular framework, the total coverage area is divided into cells. These cells are usually thought of having hexagonal geometry with the base station in the center, Figure 1, which is of course a crude approximation. In real world, base stations deployment is greatly affected by the geographic location, ease of deployment, lease or rent and other key factors. This often results in non-hexagonal geometry and sometimes, a cellular user doesn't connect to the physically nearest base station.

Today, most base stations deploy multiple directional antennas for smooth operation in a sector, as shown in Figure 2. With the combination of several antennas, a base station can steer its beam in any sector to reach out to cellular users. These antennas are known as reconfigurable antennas.

D. Reconfigurable Antenna

Until the late 19th century, there were only a few antennas utilized in mobile communication. These preliminary devices were primarily meant for experiments to show the propagation of electromagnetic waves. By mid-20th century, owing to world war II, these devices registered ubiquitous presence and later transformed the lives of an

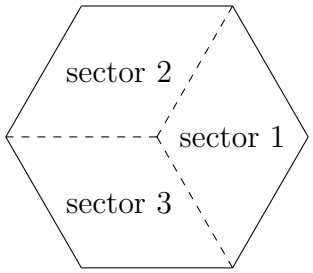

Fig. 2. A cell is further divided into three sectors each operating on different frequencies.

average person in post world war II era through radio and television signal transmission. Soon, the growth in the number of antennas in the United States were one per household which was rivaled only by then expanding auto industry during the same period.

In the 21st century, we are witnessing unparalleled growth of antennas, owing to the burgeoning mobile telecommunication market. An average person now carries at least one antenna with the cellular device (multiple if GPS is used). For distant transmission, single element antennas are sometimes unable to meet the gain or radiation pattern requirements. To meet the given assignment, sometimes combining several antenna elements in an array can produce significant increase in performance.

Antenna arrays, Radiation Pattern and Array Factor

A phased antenna array is an array of antennas in which the relative phases of the respective signals feeding the antennas are varied in such a way that the effective radiation pattern of the array is reinforced in a desired direction and suppressed in undesired direction.

A directional array is an antenna array arranged such that the superposition of the electromagnetic waves produces a predictable electromagnetic field.

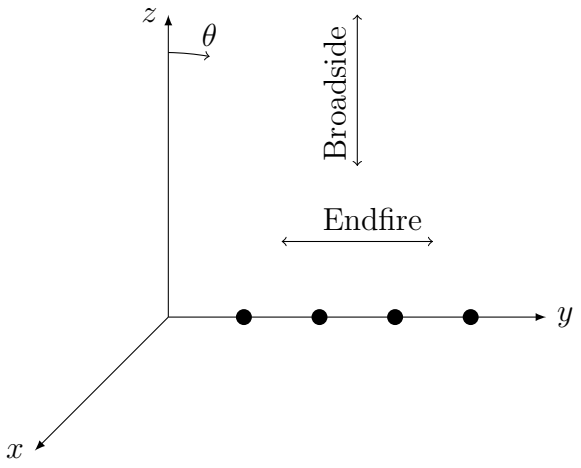

Fig. 3. Broadside vs. Endfire configuration of reconfigurable antenna.

Broadside versus End Fire Arrays

Arrays can be designed to radiate in either *broadside* fashion, i.e. radiation is perpendicular to the array orientation or *end fire* i.e. when radiation is in the same direction as the array orientation. The broadside is the z-direction and endfire is in the y-direction of the Figure 3.

E. Previous Work

The electromagnetic spectrum is a limited natural resource, and its allocation is highly regulated by authorities in different parts of the world. In the current rapidly evolving wireless ecosystem, the available radio spectrum is playing a decisively constraining role more than ever. A large portion of the assigned license spectrum is used sporadically. Consequently, a large portion of the spectrum remains underutilized. According to the Federal Communications Commission [8], temporal and geographical variations in the utilization of the assigned spectrum range from 15% to 85%. A more efficient usage of spectrum is sought to avoid a further increase in access

to licensed spectrum for mobile services. While the use of dedicated frequencies for femtocell is pragmatic, co-channel operations give higher spectral efficiency. However, co-channel operation with existing macrocell base station engenders co-channel interference [5] and is technologically more challenging. Recent work on techniques to decrease co-channel interference focuses on power control mechanisms for femto base stations [5,9]. Methods like pilot sensing [10], hybrid frequency assignment [11], frequency switching during auto-calibration [12], are proposed to avoid interference in co-channel operations. However, these power control mechanisms are generally too complicated to be implemented at the small femto base stations.

A recent rise in wide scale deployment of femtocells has presented a situation where a macrocell cellular user is potentially obstructed by these femtocells. Moreover, femtocell deployment is often unplanned and hence for smooth functioning, tracking of femtocells is required. But this additional responsibility on macrocell makes the already cumbersome task of tracking cellular users harder. Therefore an on-the-fly scheme for the detection of a proximate cellular user by a femtocell is required independent of macrocell base station. We take a novel approach and exploit the properties of a reconfigurable antenna deployed at the macrocell base station to detect nearby cellular users and avoid downlink interference from a femtocell to the macrocell base station.

F. Problem Statement

In our framework, we assume that the femtocell-to-femtocell interference is negligible as they are located far apart and do not cause any significant obstruction. Moreover, we assume that a transmitting femtocell base station does not interfere with the macrocell uplink traffic. This follows from the fact that the distance between the

cellular user and the macrocell base station is typically much greater than the distance between the femtocell base station and its users. However, the converse may not be true. A transmitting femtocell can create severe obstruction/interference to the downlink traffic of a cellular base station when the intended user is located close to the femtocell access point. In such cases, the femtocell access point should carefully choose its transmission parameters to minimize interference.

We employ a scheme where femtocell users gather data by sensing the power intended for a cellular user, which is close enough to be in the range of the femtocell base station. Naturally, a femtocell can perform better if it has knowledge of the existing network, but such an information exchange between the macrocell and femtocell tier leads to large overhead signaling and network congestion. Therefore, in this work, we are interested in the case where a femtocell has very little knowledge of the underlying cellular network.

G. Thesis Contribution

To cope up with the problem of increased interference in co-channel deployment of femtocells, this thesis defines a detection scheme for a femtocell which helps in identifying a proximate cellular user. While tracking of femtocells is pragmatically possible, it causes an extra overhead to macrocell for exchange of information. This detection scheme takes leverage of the serving user population of the femtocell and the agility of reconfigurable antenna of the existing macrocell. It equips the femtocell with the cognitive ability of discerning a potentially obstructed user without the help of existing macrocell of the sector. This scheme is tested on a Wi-Fi testbed with several Android devices playing the role of femtocell users and a reconfigurable Wi-Fi antenna. Finally, we discuss some important results obtained from the two

experiments.

CHAPTER II

SYSTEM MODEL & DETECTION SCHEME

The original voice-centric homogeneous cellular infrastructure consisting only of macrocells lacked in covering a sector, refer Figure 4, fully due to penetration loss, multipath fading, path attenuation and other factors. In emerging data-centric heterogeneous cellular networks, femtocells are deployed to overcome these problems. These small base stations provide better coverage and improved service to their respective subscribers. However, these femtocells are generally user-deployed and are often installed in an unplanned fashion, leading to increased number of hand-offs and cross-tier interference. If we consider ideal hexagonal cells, we can easily see that the signal strength on the outer boundaries of a cell becomes weaker and weaker due to path attenuation. A femtocell which is installed on the boundaries of a sector to improve coverage can produce detrimental effects to a nearby cellular user. Such a situation can be seen in Figure 5. If the power level sensed by a cellular user from a signal originating from the macrocell base station is approximately same as the power level of a signal originating from a nearby femtocell, the cellular user may experience interference. In this chapter, we present our system model which is composed of femtocells and a central macrocell base station. Together with the macrocell equipped with agile reconfigurable antenna, we propose a solution to bring down the cross-tier interference in the downlink scenario.

A. System Model

We consider a two-tier cellular infrastructure consisting of a traditional cellular base station and a set of uncoordinated femtocell access points. These femtocells are located far apart from each other, so we can safely assume that the co-tier interference

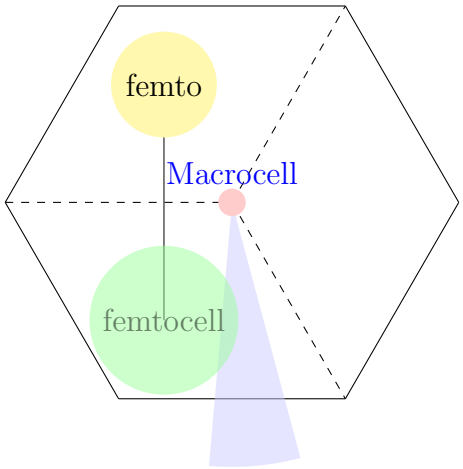

Fig. 4. A sector shown here with a unidirectional antenna and femtocells.

between these femtocells is negligible. We also assume that macrocell base stations are equipped with adaptive antenna technologies, such as phased array or reconfigurable antennas, to serve their respective user population. These base stations have priority access over the radio resources and they can perform joint scheduling to maximize network utility. In contrast, the femtocells function as subordinates to the macrocell base station and act opportunistically seeking to deliver best-effort traffic to their subscribers without creating any undue interference to the macrocell base station.

A cellular base station, when equipped with directional antenna, can pinpoint the location of a user. The directional antenna illuminates the corresponding region with a tracking beam which is typically narrow in width and has high gain, making it theoretically possible to detect the location of an active neighboring user by sensing the power level of a signal intended for the specified user. However, there are some restrictions, such as multipath fading, which complicates the situation. Mulipath fading is a propagation phenomenon, where radio signals arrive at the receiving antenna via two or more paths. This can be caused by atmospheric ducting, ionospheric

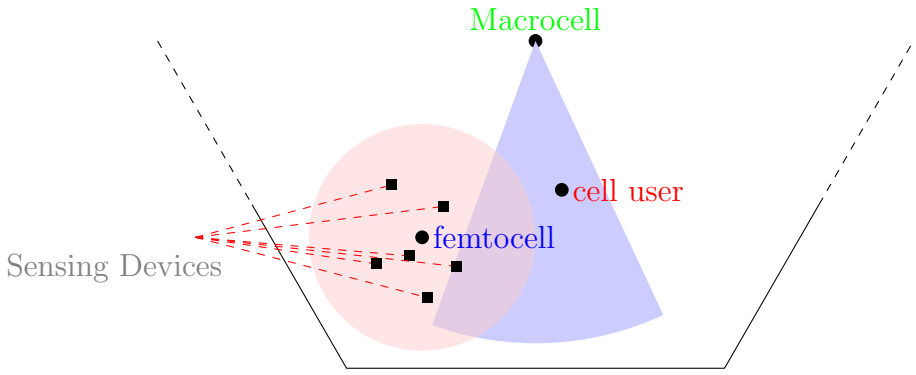

Fig. 5. A femtocell in the vicinity of a Macrocell.

reflection, reflection from large water bodies or reflections from large terrestrial objects such as nearby buildings or mountains. It prevents an accurate reading of the signal power level by a nearby sensor unit because of possible changes in phase or amplitudes, ultimately leading to constructive or destructive interference [13–15].

Fortunately, in case of femtocell this can be overcome by using the time honored strategy of averaging. Indeed, the set of devices attached to a femtocell can collectively perform the required inference task and thereby provide precise results [16, 17]. In a nutshell, a narrow beam originating from the base station can better perform the task of discrimination and can produce enhanced resolution in the location estimates.

The footprint of a femtocell is typically very small compared to that of a macrocell base station. Therefore, we can assume that all the femtocell users face approximately the same large-scale path attenuation for a sensed signal. Of course, multipath fading will vary in case of each femtocell user.

Mathematically, let $x(t)$ be the transmitted signal by the macrocell base station. If we assume that the bandwidth of this signal is much smaller than the reciprocal of the delay spread, then the signal will be subject to flat fading and can therefore be

written as

$$y(\ell, t) = \sqrt{g(\ell)} H(\ell) x(t) + w(t) \tag{2.1}$$

where ℓ is the distance from the macrocell base station to the individual femtocell user, $g(\ell)$ is the mean path attenuation, $H(\ell)$ is a random component that represents the small-scale variations due to fading, $w(t)$ is additive white Gaussian noise. We denote the distance between the femtocell base station and the macrocell base station by ℓ_{fc}. Since the distance between the femtocell base station and its users is very small compared to that between the macrocell and the femtocell, ℓ can be well approximated by ℓ_{fc}. Thus, we can write

$$y(\ell, t) \approx \sqrt{g(\ell_{\text{fc}})} H(\ell) x(t) + w(t). \tag{2.2}$$

Let ℓ_i denote the locations of the femtocell user i. When these users are more than a carrier wavelength apart, we can assume that their fading coefficients $H(\ell_i)$ are independent. Then, as the number of sensing devices increases, we get

$$\begin{aligned} \hat{y}(\ell, t) &= \frac{1}{n} \sum_{i=1}^{n} y(\ell_i, t) \\ &= \sqrt{g(\ell_{\text{fc}})} \left(\frac{1}{n} \sum_{i=1}^{n} H(\ell_i) \right) x(t) + \frac{1}{n} \sum_{i=1}^{n} w_i(t) \\ &= \sqrt{g(\ell_{\text{fc}})} \overline{H} x(t) + \overline{w}(t) \to \sqrt{g(\ell_{\text{fc}})} \mathrm{E}[H] x(t), \end{aligned} \tag{2.3}$$

where the arrow signifies an approximation in the limit of a large number of users. Thus, when $x(t)$ is known, the channel gain at location ℓ_{fc} can be estimated using the collection of devices attached to the femtocell,

$$\hat{g}(\ell_{\text{fc}}) \approx \frac{\|\hat{y}(\ell, t)\|^2}{(\mathrm{E}[H])^2 \, \|x(t)\|^2}. \tag{2.4}$$

B. Detection Theory

Detection theory deals with quantifying the ability to discern between information bearing signals and background noise signals, which are often unwanted and distract from the real signal. According to this theory, there are many determiners for detecting a signal, and where its threshold will lie.

In an interference problem, we are usually provided with an outcome Y of a random experiment which depends on an unknown parameter θ. This observation provides partial information about parameter θ. More often than not, the relation between θ and the observation Y is probabilistic rather than direct. That is, many values of θ can produce the same observation Y, but probability of producing this same result may vary according to θ.

An interference problem becomes a detection problem if the underlying attribute set, which is a set of all admissible values of θ denoted as U, can be partitioned into a finite number of subsets, and the objective is to determine to which these subsets θ belongs to. These different partitions are known as hypotheses and are labeled as $H_1, H_2, ..., H_M$. The subset of U that contains the parameter θ is called the *true hypothesis*, which we represent by H. The hypothesis $\hat{H}$ that is selected by observing Y is called *admitted hypothesis*. For a specific realization of Y, a successful detection occurs whenever $\hat{H}(y) = H$; otherwise, the detector is in error and $\hat{H}(y) \neq H$.

Binary Detection

In case of binary detection, the attribute set U can be partitioned into two subsets H_0 and H_1 commonly labeled as *null hypothesis* and *alternate hypothesis*, respectively. This is the simplest form of a detection problem, where the goal is to determine whether there is a signal present or not. In mathematical form, this translates to dis-

tinguishing between the corresponding two hypotheses. The null hypothesis typically corresponds to a general or default position. In our case, H_0 (H_1) negates (asserts) the presence of a proximate cellular user.

It is important to note that null hypothesis can never be proven or accepted. A detection test either rejects or fails to reject the null hypothesis. Table I sums up relation between the four possible outcomes of the detection test.

	H_0 is true	H_0 is false
Reject null hypothesis	False positive/False alarm	True positive
Fail to reject null hypothesis	True negative	False negative/Miss

Table I. Possible outcomes of a detection test

Type I and Type II errors

A type I error, sometimes called error of the first kind, occurs when the underlying hypothesis (null hypothesis, H_0) is true, but it is rejected. It is asserting something that is absent, a false alarm. A type II error, or sometimes called error of the second kind, occurs when the null hypothesis is false, but it is not rejected. It is failing to observe what is present, a miss.

In our current scheme, a false alarm is asserting the presence of a cellular user (rejecting H_0) when there is none. A miss, on the other hand, is negating the presence of a cellular user when actually there is one. The probabilities associated with these

events are

$$\begin{aligned} \alpha = &\quad \Pr(\text{Type I error}) &&= P(\hat{H} = H_1 | H_0) \\ \beta = &\quad \Pr(\text{Type II error}) &&= P(\hat{H} = H_0 | H_1) \\ \text{Power} = &\quad 1 - \beta &&= P(\hat{H} = H_1 | H_1) \end{aligned}$$

where $\hat{H}$ is the accepted hypothesis. The value of α is also known as *significance level of a test*. It is the probability of incorrectly rejecting the null hypothesis known as the false positive rate. *The power of a test* is defined as the probability of correctly rejecting the null hypothesis, that is not committing the type II error. *A critical value* or a threshold is the value corresponding to a given significance level. This value determines the boundary between the samples that leads to rejection of null hypothesis and the samples which lead to a decision not to reject the null hypothesis.

Minimizing errors of decision is not a simple issue. For any given sample size, the effort to reduce one type of error generally results in increasing the other type of error. The only way to minimize both types of error without refining the test is to increase the sample size; this may not be feasible.

C. Employed Detection Scheme

Consider the noted Rayleigh fading model, which captures the effects of the propagation channel on the received signal in a heavily built-up urban environment. This model asserts that the amplitude of the received signal will vary randomly according to a Rayleigh distribution.

$$f_H(h) = 2he^{-h^2}, \quad h \geq 0.$$

Note that this fading distribution is normalized to have unit power. For the sake of simplicity and accounting for modeling error, we assume that a cellular user is scheduled only when its current fade level lies between the 80th and 95th percentiles. This implies that $H(\ell_{\mathrm{r}}) \in (1.27, 1.73)$.

For a given target power P (or SNR) at the destination, this leads to the following engineering guideline. Roughly speaking, in a cellular environment, the transmit power at the base station will be such that the target power is met with equality,

$$\|x(t)\|^2 = \frac{P}{g(\ell_r)\left(H(\ell_{\mathrm{r}})\right)^2}. \tag{2.5}$$

Our previously derived bounds on $H(\ell_{\mathrm{r}})$ result in a constraint on the power of the transmit signal,

$$\|x(t)\|^2 \in \left(\frac{0.334P}{g(\ell_r)}, \frac{0.621P}{g(\ell_r)}\right). \tag{2.6}$$

When a cellular user is located in close proximity of the femtocell, we get $g(\ell_{\mathrm{r}}) \approx g(\ell_{\mathrm{fc}})$ and, necessarily,

$$\begin{aligned} \|\hat{y}(\ell_{\mathrm{r}}, t)\|^2 &\in \left(0.334P\left(\mathrm{E}[H]\right)^2, 0.621P\left(\mathrm{E}[H]\right)^2\right) \\ &= (0.262P, 0.488P) = \mathcal{S}_P. \end{aligned} \tag{2.7}$$

Conversely, when $\|\hat{y}(\ell_{\mathrm{r}})\|^2 \notin \mathcal{S}_P$, we gather that $g(\ell_{\mathrm{r}})$ must differ substantially from $g(\ell_{\mathrm{fc}})$ and, hence, the corresponding user is not located in proximity of the femtocell. When no cellular users are detected within the vicinity of the femtocell, then the access point can opportunistically seize the corresponding spectral bandwidth to serve its current subscribers.

Several factors impact the overall performance of the opportunistic scheme described above. A partial list of these factors includes the beam-widths of the high-performance antenna arrays employed by the cellular base stations, as well as the power lost in side lobes; the number of femtocell devices that are able to contribute

to the joint sensing activities; the rate at which scheduling takes place within the cellular infrastructure; user density within the cellular network; and the typical size of a femtocell. A systematic study of these elements is beyond the scope of this thesis. Still, it is important to stress that there exists a natural tradeoff between the probability of a false negative and the rate at which a femtocell access point can serve its users. In particular, the use of a guardband around $\mathcal{S}_P$ will decrease the probability of undue interference to cellular users, while necessarily diminishing the femtocell access point's ability to transmit data.

An advantage of the proposed scheme, whereby femtocells opportunistically grab spectral bandwidth when no local users are detected, is that it requires little coordination between a mobile operator and its femtocells. For instance, the femtocells need not know schedules in advance and they need not have comprehensive channel state estimates for cellular users [18]. Each femtocell only relies on static information and the data provided by its own subscribers. Furthermore, when femtocells are deployed in areas of low cellular coverage, they become unlikely to hinder the operation of the cellular network.

CHAPTER III

METHODOLOGY

In Chapter II, we proposed our framework and the system model our problem. An important part of this setup is the dynamic antenna. For our purpose, a reconfigurable antenna is composed of an array of directional antennas. This array of directional antennas is capable of changing its direction from broadside to endfire, as discussed in Section D. A setup of three directional antenna array is examined. Due to constructive interference at the center and destructive interference at a minor deviation from the central line, the antenna can emanate a high gain beam of narrow width.

Figure 6 shows a macrocell with a narrow beam of high gain, whose power is restricted to angle θ. We model the power profile of gain of the reconfigurable antenna as a function of the angle θ from the center of the beam to the exterior, and the displacement ℓ from the macrocell base station. It is well known that power decay is inversely proportional to an exponent of the distance from the origin, i.e., a macrocell base station in our case. Mathematically, it can be written as,

$$\text{Power}(\theta, \ell) \propto \frac{1}{\ell^{\alpha}}. \tag{3.1}$$

In absence of a medium, the constant α is equal to 2. For typical environments it is nearly 3 because power dissipation is more rapid due to surroundings, penetration losses, and other factors. Observing the fact that the gain of a transmitter decays greatly as the beam spreads out, it is only reasonable to assume that it decays exponentially. For a fixed θ the equation can be written in the form of

$$\text{Power}(\theta, \ell) \propto \exp(-\beta\theta^{k}), \tag{3.2}$$

where $k \geq 2$, to simulate a narrow beam of high gain around the center. For the sake

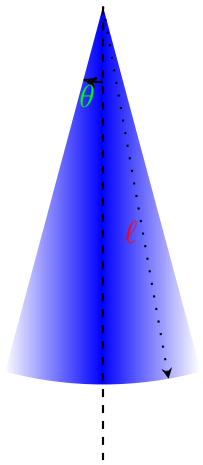

Fig. 6. Power profile of the beam as a function of θ and ℓ.

of simplicity, we keep $k = 2$. For a fixed ℓ, we get

$$\text{Power}(\theta, \ell) \propto \exp\left(-\frac{\theta^2}{\theta'}\right). \tag{3.3}$$

Which gives us the final far-field relation,

$$\text{Power}(\theta, \ell) = \frac{1}{\|\ell\|^3} \exp\left(-\frac{\theta^2}{\theta_0}\right), \tag{3.4}$$

where the essence of the proportionality constant is captured in θ_0.

A. Simulation

Recall our expression for the received signal strength found in 2.1, where two main components of the received signal are gain and fading of the signal. While we modeled the fading as Rayleigh, no such model was postulated for gain for theoretical consideration. However, for recording sensed power level, a model for gain is required which is provided by the last equation. Despite being quite specific in nature, this model provides enough insight to carry out a simulation of a real world situation.

The equation carries a constant θ_0 which needs to be determined for it to be useful. In order to find out θ_0, we look at angle θ^* where the amplitude of the beam drops to one-half of its peak value for angle $\theta = 0$. Then, it becomes quite easy to find θ_0 by the equation,

$$\frac{1}{\|\ell\|^3} = 2\frac{1}{\|\ell\|^3}\exp\left(-\frac{\theta^{*2}}{\theta_0}\right), \tag{3.5}$$

$$\text{or,} \quad \ln 2 = \frac{\theta^{*2}}{\theta_0}, \tag{3.6}$$

$$\text{or,} \quad \theta_0 = \frac{\theta^{*2}}{\ln 2}. \tag{3.7}$$

Figure 7 presents a system with a reconfigurable pattern consisting of three unidirectional antennas, each half-a-wavelength (1/3 m) apart. The receiver is placed at 200 meters (600×a-wavelength) from the central transmitter. The receiver receives signals from all three transmitters, with two of the waves from the transmitters on either side of the central transmitter, carrying a phase difference of $2\pi\nu(\|\vec{T_1} - \vec{R_0}\| - \|\vec{T_2} - \vec{R_0}\|)/c$, where $\|\vec{T_1} - \vec{R}\| - \|\vec{T_2} - \vec{R}\|$ is the path difference of the waves with respect to the wave originating from the central transmitter. This path difference (and hence the phase difference) changes once the receivers move. At any arbitrary point $\vec{R_x}$ as shown in Figure 8, the phase difference is $2\pi(\|\vec{T_1} - \vec{R_x}\|)$. So, the amplitude at the point $\vec{R_x}$ is given by $\sqrt{a^2 + b^2}$.

$$a\sin\theta + b\sin\theta \;\; = \sqrt{a^2 + b^2}\sin\left(\theta + \arccos\left(\frac{a}{\sqrt{a^2 + b^2}}\right)\right). \tag{3.8}$$

Figure 9 shows the magnitude of the power profile at a distance $\ell = 200m$. It shows a peak in the amplitude at R_0 and a sharp decline on either side of it, the type of graph one expects in case of interference.

As discussed, any detection scheme has three components: miss, detection and

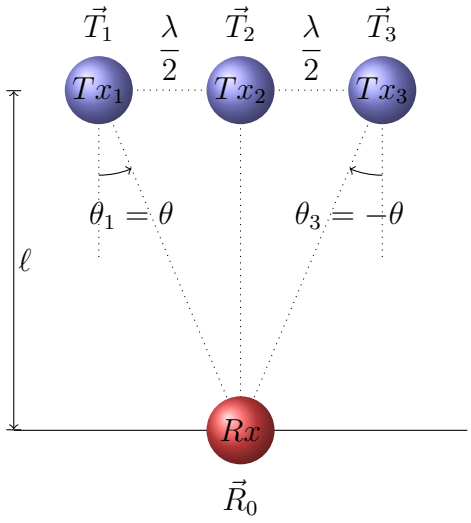

Fig. 7. A reconfigurable antenna with three unidirectional antennas and a receiver at a distance ℓ from the central antenna.

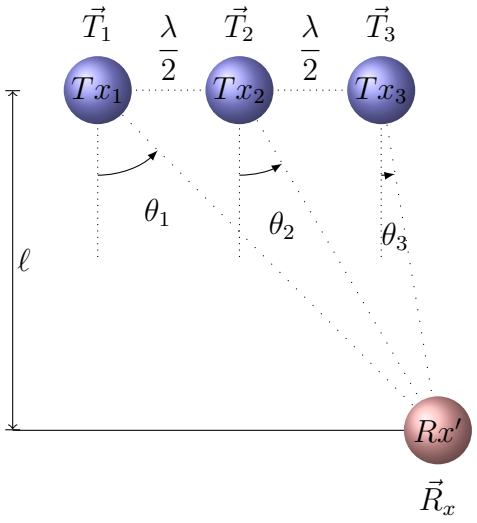

Fig. 8. Movement of the receiver in either direction inflicts a change in path difference and hence a change in phase difference.

false alarm. We are trying to minimize the probability of false alarm. In this case, false alarm can be observed due to extraordinary increase in noise power such that it is observed in the S_p interval. More often than not, background noise tends to be very weak and hardly reaches the power level to tick the alarm off. Another source of false alarm can be detection of a user who is not present in the range of the femtocell access point, but the power level registered by the femtocell users suggests otherwise. Then the question arises; how close to the femtocell access point is close enough? To solve this problem, we assume there is a guard band around the femtocell range. Any active cellular user within this guard band is treated as a potentially thwarted user. Any user outside this boundary is virtually non-existent to the femtocell base station. The former case of potentially obstructed cellular user is shown in Figure 10 and the latter case is shown in Figure 11.

Table II lists variables used in the algorithm 1 and their values. The chosen values

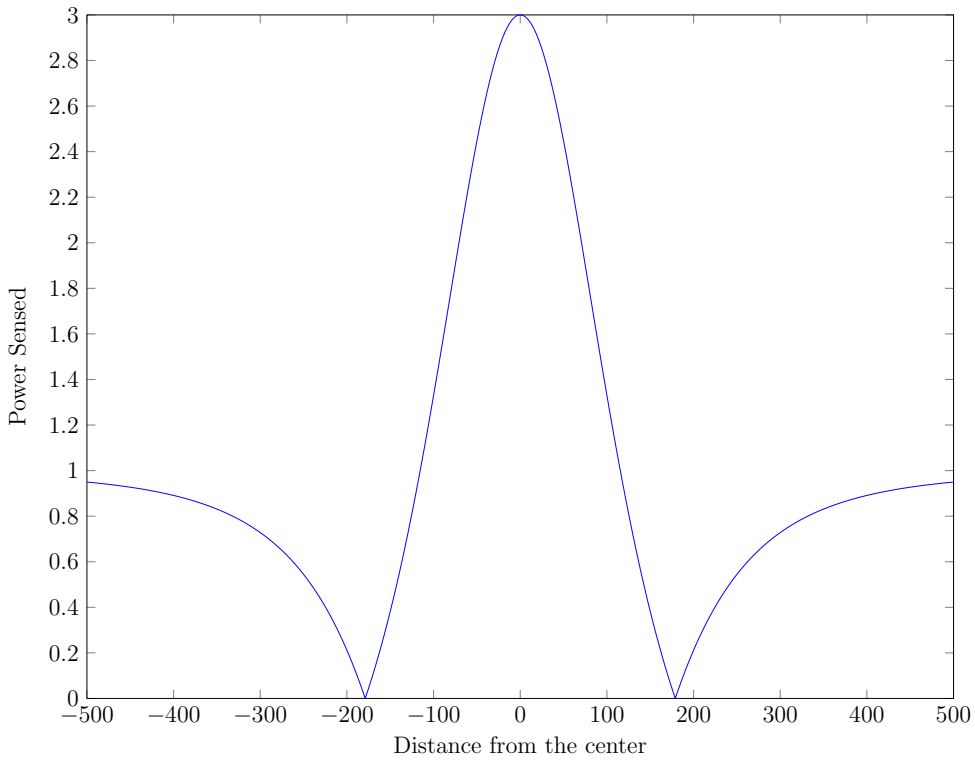

Fig. 9. Power profile of gain as a function of angle θ for three transmitters and a receiver, with a fixed distance ℓ from the central antenna.

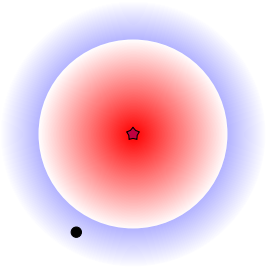

Fig. 10. Miss: when there is an actual cellular user but reported as none.

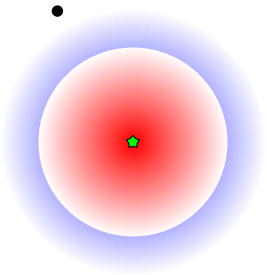

Fig. 11. False alarm: when there is no cellular user but reported as a cellular user in sight.

Variable	Notation	Value
Velocity Constant	c	3×10^8 m/s
Frequency	ν	900 MHz
Wavelength	λ	$\lambda = c/\nu = 1/3$ m
Receiver Position	R	(0, 600λ)= (0,200)
Antenna 1 Position	T_1	(-1/6,0)=(-λ/2,0)
Antenna 2 Position	T_2	(0,0)
Antenna 3 Position	T_3	(1/6,0)=(λ/2,0)

Table II. Variables used in algorithm to determine θ_{req}.

are typical and are frequently observed in cellular networks. The position of the three antenna for calculating θ is heuristically similar to real world, if not accurate.

Algorithm 1 Simulation to find power profile

$\lambda \leftarrow \frac{c}{\nu}$

$T_1 \leftarrow \left(\frac{-\lambda}{2}, 0\right)$, $T_2 \leftarrow (0,0)$, and $T_3 \leftarrow \left(\frac{\lambda}{2}, 0\right)$ {Define the position of the three transmitters}

$R \leftarrow (0, -r)$ {Define the position of the receiver}

$\theta_1 \leftarrow \arcsin\left(-\sin\left(\frac{2\pi\nu}{c}(\|T_1 - R\| - \|T_2 - R\|)\right)\right)$

$\theta_3 \leftarrow \arcsin\left(-\sin\left(\frac{2\pi\nu}{c}(\|T_3 - R\| - \|T_2 - R\|)\right)\right)$

for $i = 0$ **to** 20000λ **do**

  $R_x \leftarrow (i, -r)$

  $P_1 \leftarrow \theta_1 + \frac{2\pi\nu}{c}\|T_1 - R_x\|$

  $P_2 \leftarrow \frac{2\pi\nu}{c}\|T_2 - R_x\|$

  $P_3 \leftarrow \theta_3 + \frac{2\pi\nu}{c}\|T_3 - R_x\|$

  $\sigma(i) \leftarrow \sqrt{(\sin(P_1) + \sin(P_2) + \sin(P_3))^2 + (\cos(P_1) + \cos(P_2) + \cos(P_3))^2}$

end for

$I \leftarrow$ Index of first non-zero element such that $\frac{\sigma}{\sigma(1)} < 0.5$

$x_{req} \leftarrow x(I)$

$\theta_{req} \leftarrow \arctan\left(\frac{x_{req}}{\|R\|}\right)$

Theoretically, the receiver should move in a circle around the central antenna, but the change in radius is negligible relative to the change in the angle. Through algorithm 1, we are able to find the right θ^* where the value of the amplitude halves.

Algorithm 2 aims at finding the right guard band width. Logically, the width of the guard band has to be less than the range of the femtocell base station. Therefore, we consider all the possible guard bands around the range of the femtocell, and a cellular user sitting on the circumference of this circle of radius ℓ_{FC}. The femtocell range need not be circular in nature, yet it is often approximated to be a circle of a given radius to make calculations easy. Another important point to notice is that although, in theory it is possible that a cellular user could be in the shaded region, as shown in Figure 12, practically this would not happen. Hence, it is reasonable to assume that the cellular user is between the range 120° to 240°.

Variables	Notation	Value
Power	P	-82 dBm
Power Spectral Density	PSD	-160 dBm/Hz
Bandwidth	bw	54 MHz
Upper Percentile	p_u	95
Lower Percentile	p_l	80
Location of Radio Base Station	ℓ_{RBS}	(-150,0)
Location of Femtocell Base Station	ℓ_{FC}	(0,0)
Radius of femtocell coverage	d	50
Number of Femtocell Users	FemtoUE	8

Table III. Variables used in algorithm 2 & 3.

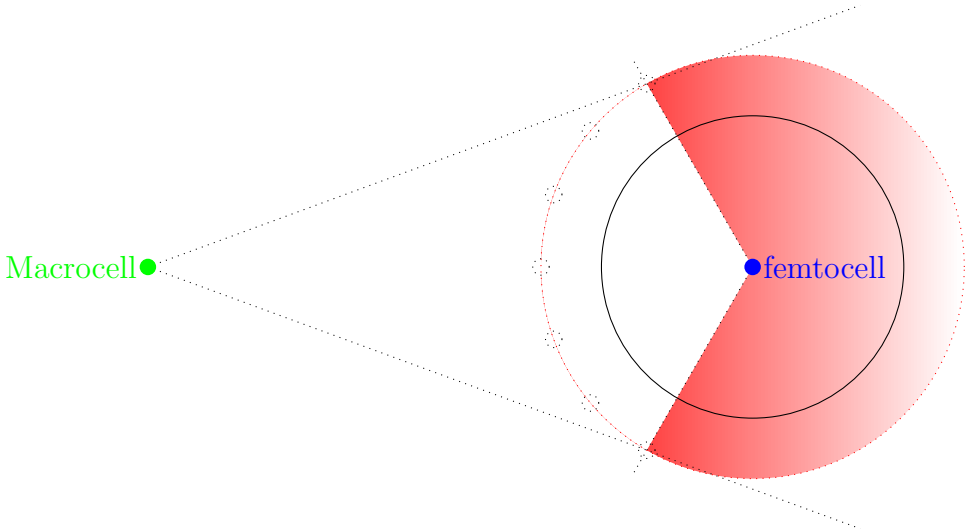

Fig. 12. Simulation setup.

In this algorithm, we assume that, even if the cellular user is on the guard band and is detected as an active user, this event counts as a false alarm. For each possible location of a cellular user on the circumference, femtocell users are generated with random location inside the coverage area.

Algorithm 2 Simulation to find Probability of error

Require: P, PSD in Watts, $0 < p_l < p_u < 1$, $bw, \theta_{req}, \vec{d}, \vec{\ell}_{FC}, \vec{\ell}_{RBS}, FemtoUE$

1: $b_l \leftarrow -\frac{\pi}{4}\frac{P}{\log(1-p_u)}$
2: $b_u \leftarrow -\frac{\pi}{4}\frac{P}{\log(1-p_l)}$
3: $\sigma \leftarrow \sqrt{PSD \times bw}$
4: $\theta_0 = \frac{\theta_{req}^2}{\log 2}$
5: **for all** GuardBand radius in $(50, 55, ..., 100)$ **do**
6: **for all** Location of Primary User at Guardbands **do**
7: **for all** Number of Trials **do**
8: **for all** Users i in $(1, ..., FemtoUE)$ **do**
9: Generate random locations of femtocell users inside the femtocell base station coverage circle of radius ℓ_{FC}
10: $\vec{t_1} \leftarrow \vec{\ell}_{FC} - \vec{\ell}_{RBS}$, $\vec{t_2} \leftarrow \vec{\ell}_{PU} - \vec{\ell}_{RBS}$
11: $t = \angle\vec{t_1} - \angle\vec{t_2}$
12: Gain for User $G_i \leftarrow \frac{1}{\|\ell_{FC} - \ell_{RBS}\|^3} \exp(-t^2/\theta_0)$
13: **end for**
14: $G_r \leftarrow \frac{1}{\|\ell_{PU} - \ell_{RBS}\|^3}$
15: $y \leftarrow \sqrt{\frac{P}{G}} 1.5174 \sum \sqrt{G_i} \frac{Rayleigh(\frac{1}{\sqrt{(2)}}, UE)}{UE} + \sigma * \frac{N(0,1)}{UE}$
16: **if** $b_l < y^2 < b_u$ **then**
17: falseAlarm++
18: **end if**
19: **end for**
20: Normalize falseAlarm by falseAlarm $\leftarrow$ falseAlarm/Number of Trials
21: **end for**
22: **end for**

The gain for every user and the cellular user is calculated based on the (3.4). An extra term appears on the line 15 of algorithm 2, 1.5174, which corresponds to $E[H|h \in (80, 95)]$. Table III lists variables used in the algorithm 2 and 3 and their

values. These values are typical and are frequently observed in cellular networks.

The probability of false alarm is simulated for a fixed number of femtocell users. The result suggests that the percentage of false alarm goes down as the cellular user drifts away from the femtocell coverage area. Therefore, for a better resolution of a cellular user, a large guard band width is preferable. But at the same time, a large guard band can be prejudicial to the femtocell users. Hence, selection of guard band is a trade off between lowering the percentage of false alarm and minimizing the guard band width. This guard band is chosen to be additional 20 m for a femtocell with coverage area of 50 m.

Having chosen a width for the guard band, we made some minor changes in algorithm 2 to come up with algorithm 3. Algorithm 3 works along the same principle but with minor tweak to record received signal strength.

Algorithm 3 Simulation to find Probability of error

Require: P, PSD in Watts, $0 < p_l < p_u < 1$, $bw, \theta_{req}, \vec{d}, \vec{\ell}_{FC}, \vec{\ell}_{RBS}, FemtoUE$

$b_l \leftarrow -\frac{\pi}{4}\frac{P}{\log(1-p_u)}$

$b_u \leftarrow -\frac{\pi}{4}\frac{P}{\log(1-p_l)}$

$\sigma \leftarrow \sqrt{PSD \times bw}$

$\theta_0 = \frac{\theta_{req}^2}{\log 2}$

for all $NumUE$ in $(1, .., FemtoUE)$ **do**

  GuardBand radius $\leftarrow GB^*$

  for Location of Primary User at Guardbands in $[2\pi/3, 4\pi/3]$ **do**

    for all Number of Trials **do**

      for all Users i in $(1, ..., FemtoUE)$ **do**

        Generate random locations of femtocell users inside the femtocell base station coverage circle of radius ℓ_{FC}

        $\vec{t_1} \leftarrow \vec{\ell}_{FC} - \vec{\ell}_{RBS}$, $\vec{t_2} \leftarrow \vec{\ell}_{PU} - \vec{\ell}_{RBS}$

        $t = \angle\vec{t_1} - \angle\vec{t_2}$

        Gain for User $G_i \leftarrow \frac{1}{\|\ell_{FC} - \ell_{RBS}\|^3} \exp(-t^2/\theta_0)$

      end for

      $G_r \leftarrow \frac{1}{\|\ell_{PU} - \ell_{RBS}\|^3}$

      $y \leftarrow \sqrt{\frac{P}{G}} 1.5174 \sum \sqrt{G_i} \frac{Rayleigh(\frac{1}{\sqrt{(2)}}, FemtoUE)}{FemtoUE} + \sigma * \frac{N(0,1)}{FemtoUE}$

      if $b_l < y^2 < b_u$ **then**

        falseAlarm++

      else

        miss++

      end if

    end for

    Normalize falseAlarm by falseAlarm $\leftarrow$ falseAlarm/Number of Trials

    Normalize miss by miss $\leftarrow$ miss/Number of Trials

  end for

end for

This algorithm is run for the number of femtocell users ranging from 1 to 12, and the results produced are shown in Figure 13. This figure also illustrates the probability of miss calculated through algorithm 3.

Figure 13 shows the probability of a false negative as a function of the number of devices in the femtocell. For illustrative purposes, the decision rule is simply taken

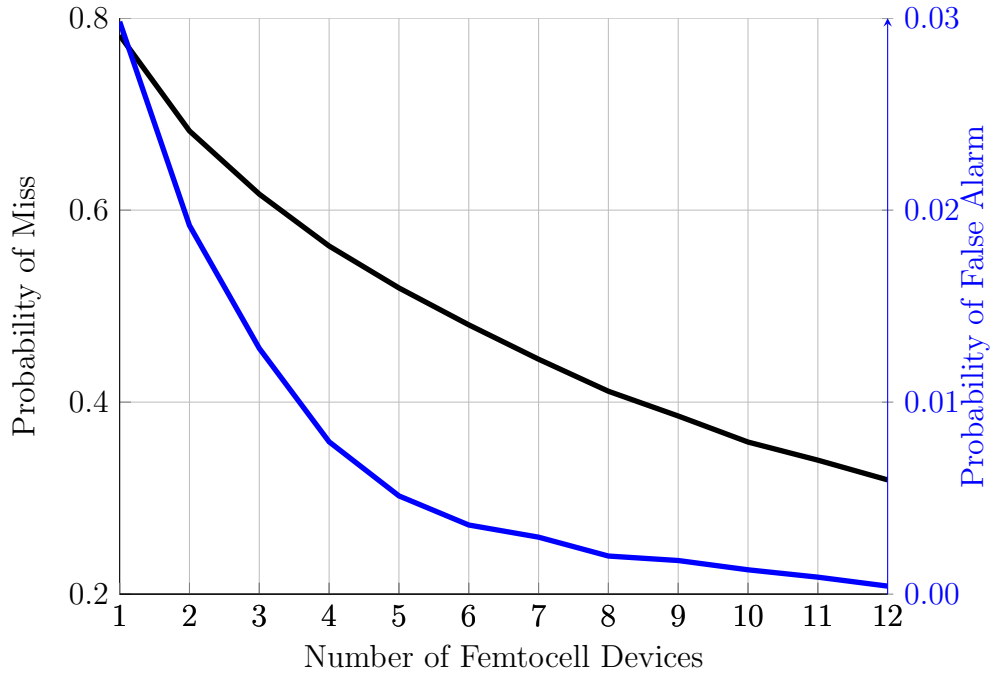

Fig. 13. Performance results obtained through Monte-Carlo Simulations.

to be

$$\mathrm{D}\left(\{y(\ell_i,t)\}\right) = \begin{cases} \text{user nearby} & \|\hat{y}(\ell_{\mathrm{fc}},t)\|^2 \in \mathcal{S}_P \\ \text{user elsewhere} & \|\hat{y}(\ell_{\mathrm{fc}},t)\|^2 \notin \mathcal{S}_P. \end{cases} \tag{3.9}$$

In this example, the noise components $\{w_i(t)\}$ are assumed to be independent Gaussian random variables. The power spectral density (including interference) is -160 dBm/Hz, which yields a noise variance of $\sigma^2 = -102.68$ dBm; the target power is $P = -82$ dBm. These parameters have been selected to mimic the operation of a typical cellular infrastructure.

B. Experimental Setting

Preliminary testing of the framework discussed before was conducted using a Wi-Fi testbed with Android devices. The Wi-Fi access point acted as the macrocell base

station and was equipped with a custom two-state reconfigurable antenna system. This antenna can switch its configuration from broadside to endfire. The antenna used changes its spatial distribution of radiated power, but preserves its frequency response by maintaining a common impedance bandwidth. The android devices were preloaded with a custom application, which assists in recording the received signal strength of the Wi-Fi transceiver. This application was altered multiple times to gather meaningful set of data.

Android Implementation

Today smartphones carry a lot of in-built special devices such as Global Positioning System (GPS), camera, radio, gyroscope, apart from the usual two-way radio feature. Android operating system besides being open source, has implemented these features very elegantly. Access to the built-in GPS and a data network enables access to the latitude, longitude and altitude. The Android operating system also provides access to current Received Signal Strength Indication (RSSI).

A small custom Android application was created specifically for collecting observations. This application was installed onto a set of mobile devices that can simulate, collectively, the role of the femtocell subscribers. On each device, the received signal strength and service set identifier (SSID) of the Wi-Fi access point was obtained using the `WifiManager` class that is a part of the Android Software Development Kit (SDK). Similarly, locations of the femto-like sensing devices was recorded using the `LocationManager` class. A location entry helps ensure that the sensing devices do not venture past the boundary of the virtual femtocell. The outliers were simply discarded. The collected information was time-stamped and stored locally on the devices using a `ContentProvider` and the `SQLite` database. It was subsequently transferred to a `MySQL` database on an Internet server using a custom `HttpClient` interface.

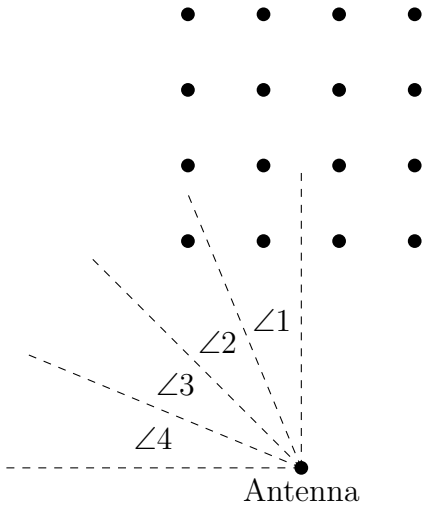

Fig. 14. Arrangement of femto devices for experiment 1, with the Wi-Fi antenna at the bottom.

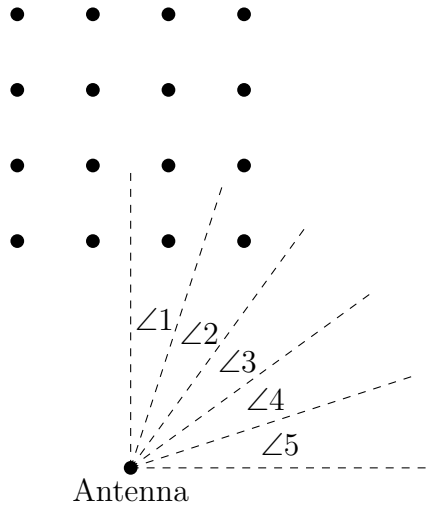

Fig. 15. Arrangement of femto devices for experiment 2, with the Wi-Fi antenna at the bottom.

It is worth noting that most GPS on smartphones use assisted GPS (A-GPS) technology, that uses satellites along with the services of marcocell base stations of the service provider to greatly improve startup performance, or time-to-first-fix (TTFF). TTFF describes the time and process required for a GPS device to acquire enough usable satellite signals and data to provide accurate navigation.

Our first venture to record the data with mobile femtocell users was unsuccessful, partly because there was no data packet service which can provide the additional support to the GPS. The smartphones were connected to a Wi-Fi access point that was disconnected from the Internet. Also connecting to a Wi-Fi interface disconnects a smartphone from the data packet service and hence location entries would not be meaningful. Without correct location entries, it was hard to discriminate between users inside and outside femtocell range, rendering the whole experiment unsuccessful.

Another set of field experiment was conducted keeping the equidistant femtocell users stationary and dropping the location entries entirely in the custom application.

The first experiment of this set was conducted by manually steering the Wi-Fi antenna to create four different configurations labeled angle 1 to 4. A total of sixteen femtocell users were used to collectively gather data as shown in Figure 14, whereas, Figure 15 shows the setup for second experiment with five configurations. These Android devices were initially connected to the Wi-Fi access point with a reconfigurable antenna. The beam was kept stationary in each configuration for a fixed amount of time and then moved to the next one. The recorded observations were time stamped and the beam was steered from angle 1 to 4. To distinguish between different configurations, a drop in sensed power level was considered along with the time spent in each configuration. Figure 16 plots different mean power for each node averaging over the time spent in each configuration.

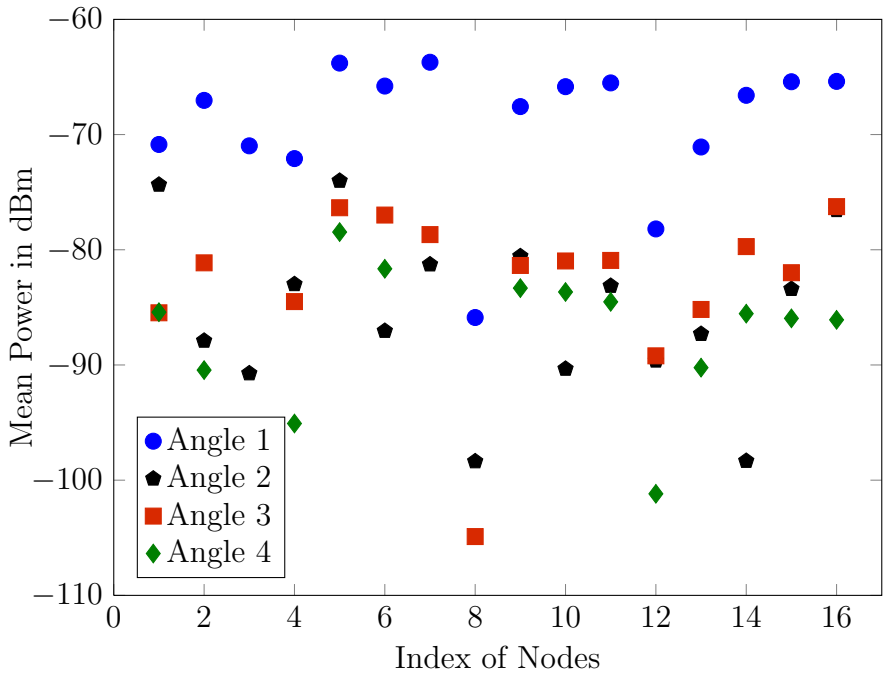

Fig. 16. Mean power obtained from the experiment 1.

The results obtained show that if the angles to be compared are far apart, it is quite easy for the femtocell to distinguish between those angles. For example, angles

1 and 4, or angles 1 and 3 are easy to distinguish from one another almost in every case, but it is hard to distinguish between the angles 2 and 3 in most cases.

The second experiment also consisted of sixteen femtocells, but for some unforseen reasons twelve of them failed to record any data. This time a reconfigurable antenna was attached to the Wi-Fi access point rather than manually steering the antenna. There were five configurations instead of four.

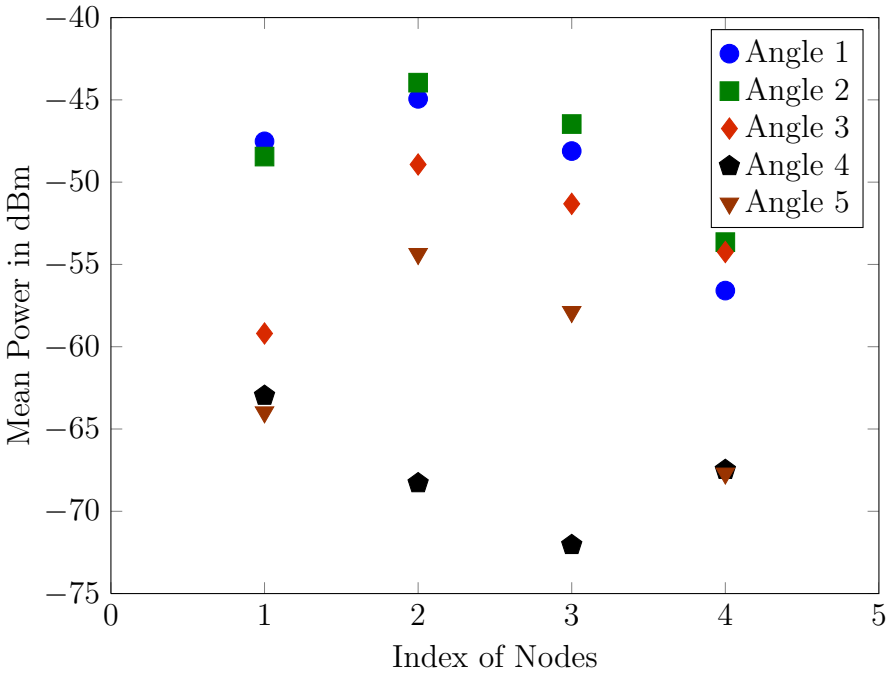

Fig. 17. Mean power obtained from the experiment 2.

The results obtained from experiment 2 are illustrated in Figure 17, which plots the mean power sensed by each femtocell user device averaged over the time spent in each configuration. The figure indicates a great degree of discernability by femtocell for those angles which are far apart. However, it again somewhat struggles to distinguish between two close angles.

Overall, it can be inferred that a femtocell using this detection scheme can make an educated decision to turn off the transmission whenever it perceives there is a

potential cellular user in its sight. The probability of error goes down very quickly if the number of femtocell users is increased.

CHAPTER IV

CONCLUSION

In this thesis, we discussed possible performance enhancements to wireless cellular infrastructures by co-channel deployment of femtocells and macrocells. Co-channel deployment with frequency reuse is indeed very efficient and profitable from the operators' perspective, but its implementation is nonetheless very challenging. To combat the co-tier interference, which is intrinsic to universal frequency reuse, we present a detection scheme that leverages the use of reconfigurable antenna provided to cellular base stations, and the collective data gathering capabilities of femtocell users, which act as a distributed power level sensing system. We assume that the uplink transmission from the cellular user to the macrocell is unperturbed by a transmitting femtocell.

The preliminary study demonstrates that subordinate femtocells may be able to detect the presence of nearby cellular user without requiring excessive side information from their service providers. This is encouraging as it offers supporting evidence to the fact that femtocells can increase the capacity of traditional cellular infrastructures in a scalable, uncoordinated manner. When femtocells are successful at detecting nearby cellular users, they can opportunistically take advantage of available spectral bandwidth without impairing the performance of the cellular system as seen by its traditional users. As a future endeavor, we plan to implement an enhanced testbed with the capacity to adapt to changing conditions in real time.

REFERENCES

[1] International Telecommunication Union, "International Telecommunication Union Statistics," Available: http://www.itu.int/ITU-D/ict/statistics, Aug. 2012.

[2] H. Claussen, L. T. W. Ho, and L. G. Samuel, "An overview of the femtocell concept," *Bell Labs Technical Journal*, vol. 13, pp. 221 - 245, 2008.

[3] B. Cetiner, E. Sengul, E. Akay, and E. Ayanoglu, "A MIMO System with Multifunctional Reconfigurable Antennas," *Antennas and Wireless Propagation Letters, IEEE*, vol. 5, no. 1, pp. 463 - 466, Dec. 2006.

[4] A. Glazunov, and P. Karlsson, and R. Ljung, "Cost analysis of smart antenna systems deployment," *Proc. VTC 2005-Spring Vehicular Technology Conf. 2005 IEEE 61st*, vol. 1, pp. 329 - 333, 2005.

[5] H. Claussen, "Performance of Macro- and Co-Channel Femtocells in a Hierarchical Cell Structure," in Proc. of *IEEE International Symposium on Personal, Indoor and Mobile Radio Communications,* pp. 1 - 5, Sept. 2007.

[6] V. Chandrasekhar, and J. G. Andrews, "Femtocell networks: A survey," *IEEE Communications Magazine*, vol. 46, no. 9, pp. 59 - 67, Sept. 2008.

[7] C. Patel, M. Yavuz, S. Nanda, "Femtocells [Industry Perspectives]," *IEEE Wireless Communications,* vol. 17, no. 5, pp. 6 - 7, Oct. 2010.

[8] Federal Communications Commission, "Notice of proposed rule making and order," ET Docket No 03-222, Dec. 2003.

[9] X. Li, L. Qian, and D. Kataria, "Downlink power control in co-channel macrocell femtocell overlay," *43rd Annual Conference on Information Sciences and Systems,*, pp. 383 - 388, Mar. 2009.

[10] T-H Kim, and T-J Lee,"Throughput Enhancement of Macro and Femto Networks By Frequency Reuse and Pilot Sensing," *IEEE International Performance, Computing and Communications Conference,* pp. 390 - 394, Dec. 2008.

[11] I. Guvenc, M-R Jeong, F. Watanabe, and H. Inamura, "A hybrid frequency assignment for femtocells and coverage area analysis for co-channel operation," *IEEE Communication Letters,* vol. 12, no. 12, pp. 880 - 882, Dec. 2008.

[12] M. Yavuz, F. Meshkati, S. Nanda, A. Pokhariyal, N. Johnson, B. Raghothaman, and A. Richardson, "Interference management and performance analysis of UMTS/HSPA+ femtocells," *IEEE Communication Magazine,* vol. 47, no. 9, pp. 102 - 109, Sept. 2009.

[13] D. Tse, and P. Vishwanath, *Fundamentals of wireless communication.* New York, NY, USA: Cambridge University Press, 2005.

[14] W. C. Jakes, *Microwave mobile communications.* Piscataway, NJ, USA: Wiley-IEEE Press, 1994.

[15] E. Biglieri, J. Proakis, S. Shamai, "Fading channels: information-theoretic and communications aspects," *IEEE Transactions on Information Theory*, vol. 44, no. 6, pp. 2619 - 2692, Oct. 1998.

[16] S. M. Kay, *Fundamentals of Statistical Signal Processing, Volume I: Estimation Theory (v.1).* Upper Saddle River, NJ, USA: Prentice Hall, 1993.

[17] D. MacKay, *Information Theory, Inference and Learning Algorithms,* New York, NY, USA: Cambridge University Press, 2002.

[18] A. Lapidoth, and P. Narayan, "Reliable communication under channel uncertainty," *IEEE Transactions on Information Theory,* vol. 44, no. 6, pp. 2149 - 2177, Oct. 1998.